IEEE Access
Multidisciplinary | Rapid Review | Open Access Journal

Received May 18, 2021, accepted June 10, 2021, date of publication June 28, 2021, date of current version July 5, 2021.

Digital Object Identifier 10.1109/ACCESS.2021.3092749

Analysis of Electromagnetic Field Distribution Generated in an Semi-Anechoic Chamber in Aspect of RF Harvesters Testing

WIESŁAW SABAT, DARIUSZ KLEPACKI, (Member, IEEE), KAZIMIERZ KAMUDA, AND KAZIMIERZ KURYŁO

Department of Electronic and Telecommunication Systems, Rzeszów University of Technology, 35-959 Rzeszów, Poland

Corresponding author: Dariusz Klepacki (dklepa@prz.edu.pl)

This work was supported in part by the Minister of Education and Science of the Republic of Poland within the ''Regional Initiative of Excellence'' Program for years 2019–2022 under Project 027/RID/2018/19, and in part by the European Union Programs under Grant POPW.01.03.00-18-012/09-00 and Grant UDA-RPPK.01.03.00-18-003/10-00.

This work did not involve human subjects or animals in its research.

ABSTRACT The results of work in the field of analysis of the distribution of electromagnetic fields generated by the antenna of an RFID reader operating in the UHF frequency band have been presented in this paper. The carried-out tests concern the efficiency of obtaining energy from the field of an electromagnetic RFID reader. To analyze the distribution of the electric field strength, the calculation procedures were elaborated on the basis of the developed mathematical dependencies in the MathCad program. The developed numerical procedures enable the synthesis of the electric field strength and power density distribution for a given antenna radiation pattern, for any suspension heights of the transmit and receive antennas and any mutual distance between them. In order to verify the correctness of calculations the test stands and measurements were made for a model antenna. The measurements were carried out in a semi-anechoic chamber.

INDEX TERMS Antennas, electromagnetic field distribution, RFID, RF harvesting.

I. INTRODUCTION

The results of the work presented in the paper concern the issue of electromagnetic harvesting and related aspects of obtaining energy from the electromagnetic field generated by the antenna of the RFID reader. Such problems have been the subject of scientific research in recent years and can be found in referenced publications [1]–[5].

The RFID reader is an element that receives data from identifiers within its operation zone as well as a source of energy supplying a given tag. The electromagnetic field generated by the reader antenna can additionally be used as an energy source for semi-passive RFID tags, as well as autonomous electronic systems, e.g. wireless sensor networks.

Considering the antenna-harvester system in single and multiple identification systems, the analysis can be limited to a one-dimensional problem (1D). In such a system, the antenna can be treated as a point source of energy and the harvester as its point receiver. This approach to the problem allows for simplification in balancing the energy that is available at a given point in space.

Path loss between the two communicating antennas strongly depends on the propagation environment and has been extensively studied in wireless communications [6]–[9]. In recent years, there were several articles with studies and analysis of propagation environment specifically in application to UHF RFID systems [9]–[14]. The analysis of selected papers has indicated that simplified analytical and numerical models may be used to analyze the signal and course propagation process. For instance, simplified analytical models are very frequently used when the value of power strength or equivalent electric field density has to be determined in selected point of space in wireless communication system. Examining the results included in papers where analytical models were used, it may be observed that the authors obtain differently correlated results of calculations and measurements [7], [8], [9], [12]. This diversity in correlation is triggered by a variety of factors related to the model, measuring procedures and the quality of equipment.

The associate editor coordinating the review of this manuscript and approving it for publication was Jie Tang.

In majority of the published papers, the measured values of the electromagnetic field strength or power density were analyzed in the real-world operating conditions of the system [7]–[12]. It allows for the determination of the elements conditioning the process of energy harvesting from the electromagnetic field. However, it does not allow for unequivocal determination of the influence of the analyzed parameter on the observed measurement result. Intending to unequivocally define the above-mentioned factors, the authors propose conducting of the such measurements in an anechoic or semi-anechoic chamber. The former will allow to determine the propagation losses in free space, while the chamber with a conductive floor - the influence of the conductive ground on the additional effect of reflection and interference of electromagnetic waves. The effects observed in the anechoic chamber are related to the effects observed in the real environment. Due to the ground surface (conductive ground, building partitions, modern finishing and facade materials), the energy received by the harvester reaching is the result of direct propagation and signal interference on many roads.

The aim of the work was to elaborate a model that would allow the calculation of the strength of the electromagnetic field and the power density at any point in the anechoic chamber on the line between the antenna and the harvester and its verification. When developing, It was assumed that the simulation model would allow for the analysis of antenna-harvester systems, in which these elements are placed in a way deviating from the classic considerations (antennas at different heights, no correlation of optical axes of the antennas, the possibility of LoS, NLoS, OLoS propagation). It was also assumed that the model would be able to analyze the real radiation pattern of antenna. In majority of analyzed publications, only its isotropic model was used in the calculations [7]–[9], [13], [14].

The realization of the research in accordance with the assumed goal required the elaboration of computational algorithms that would allow for the estimation of the of the electromagnetic field strength and the equivalent energy density at any distance from the antenna and for the given propagation conditions. Algorithms and computational procedures were developed in the Mathcad program [20] based on known dependencies available in the literature. For the selected verification antenna (Pasternack PE51054), its radiation patterns were measured in the anechoic chamber. Using the algorithm described in [21], models of radiation patterns for the analyzed antenna have been elaborated.

An automatic line scanner was built to automatically measure the distribution of the electromagnetic field generated by the model antenna, using the Innco KMS6000 test bench mechanism and control system and ETS Lintgren's HI6005 isotropic electric field probe. Using this scanner, for the selected PE51054 antenna in the 3M chamber from TDK, measurements of electromagnetic field distributions were carried out for various actual antenna settings, its operating frequency and delivered power. The analysis of the field strength distribution generated in the chamber by the PE51054 antenna was carried out for two cases. In one, the floor of the chamber was covered with TDK ISK-030A absorbers. In the second case, the metal floor of the chamber was used as an ideally reflecting surface. In addition, the analysis also took into account the influence of antenna polarization on the distribution of the generated field. The model antenna was powered by the BBA100 amplifiers by Rohde&Schwarz and the BLMA-1060 100 / 50D by Bonn, controlled by the SMF100A generator by Rohde&Schwarz. The Rohde&Schwarz EMC32 software package was used to control and stabilize the power delivered to the analyzed antenna.

The designed and constructed measuring stand allowed for the verification of the developed calculation procedures.

II. METHOD OF CALCULATING THE DISTRIBUTION OF THE ELECTROMAGNETIC FIELD IN AN ANECHOIC AND SEMI-ANECHOIC CHAMBERS

The most basic model of the distribution of the electric field around the antenna is a free-space one with an isotropic antenna. Since there is no real antenna model that would be able to emit the power with the same density in every direction, this model has only a theoretical meaning. In a communication system, each real antenna is described by specific radiation pattern and directive gain. In case of an antenna with directivity G in free space conditions, the relation between power P, supplied to the antenna, and superficial power density S of a radio wave, located within the distance r from the source is described by:

$$\mathrm{S}\,(\mathrm{r},\theta,\varphi) = S_m \cdot f_p\,(\theta,\varphi) = \frac{P \cdot G}{4\pi \cdot r^2} \cdot f_p\,(\theta,\varphi) = \frac{EIRP}{4\pi \cdot r^2} \cdot f_p\,(\theta,\varphi) \quad (1)$$

where S(r,θ, φ) indicates field's superficial power density in point (r,θ, φ) on the selected direction of transmitting antenna, S_m superficial power density amplitude, generated by isotropic antenna, $f_p(\theta, \varphi)$ – directional power antenna characteristic, G – antenna gain in linear scale, EIRP – equivalent isotropically radiated power [19].

The equivalent isotropically radiated power EIRP has practical importance. It results from the fact that the permitted power levels in telecommunications systems are determined by this quantity. When designing a system for an antenna with a given gain, we choose the value of the power delivered to the antenna so as not to exceed the permissible, equivalent power radiated isotropically by the antenna.

In engineering practice, when measuring the parameters of the electromagnetic field, antennas or a system of antennas that allow for the direct determination of the intensity of the electric field at the point of measurement are used very often. When the receiving antenna is located in the transmitting antenna far field and its surrounding space is linear and homogenous, the relation between electric field strength E(r,θ, φ) and power density is:

$$\mathrm{E}\,(r,\theta,\varphi) = \sqrt{S\,(r,\theta,\varphi) \cdot Z_f} \quad (2)$$

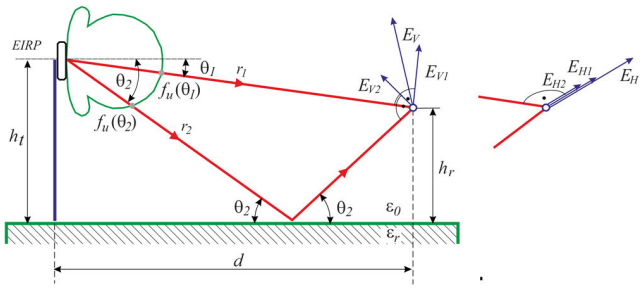

FIGURE 1. Geometry of electric field vectors for vertical and horizontal polarization.

where Z_f stands for medium's wave impedance, which for a free space equals $Z_f = 120\pi$. Given the (1, 2), the value of a maximum electric field strength on a selected radiation direction of transmitting antenna can be calculated from:

$$\mathrm{E}(r,\theta,\varphi) = E_m \cdot f_u(\theta,\varphi) = \frac{\sqrt{60P \cdot G}}{r} f_u(\theta,\varphi) = \frac{\sqrt{60EIRP}}{r} f_u(\theta,\varphi) \tag{3}$$

where $f_u(\theta, \varphi)$ is the voltage antenna pattern [3].

This assumption is correct, providing that the isotropic probe is used to measure the electric field strength.

The knowledge of antenna radiation pattern is necessary to obtain the distribution of radiated power density and electric field strength in each situation where antenna measuring probe is not located in the direction of maximum antenna radiation. These relations are very frequently applied to analyze RFID systems sensitivity and determine the level of power that can be derived from electromagnetic field of antenna reader. In this analysis, direct visibility of system elements is considered, whereas the dispersion and electromagnetic wave reflection effects are omitted.

In real environment, because of propagation of waves from ground, floor, walls or elements in the antenna's range, the field is calculated as a sum of direct and reflected waves. The direct one, reaching receiving antenna, is damped in a scale dependent on free-space parameters. The electromagnetic wave, striking on media's boundary is reflected and dispersed. The ratio of reflected and incident waves' electric field strength is called the reflection coefficient. In general scope, the coefficient is a complex number.

$$\underline{R} = |R|\, e^{-j\vartheta} \tag{4}$$

where |R| means reflectance magnitude, ϑ - phase of reflection coefficient.

In the case of a vertically and horizontally polarized wave, with perfectly flat boundary plane, reflection coefficients $\underline{R}_V$ and $\underline{R}_H$ for a given ground permeability ε_r as a function of the angle of elevation θ are determined by the following relations [20]:

$$\underline{R_V} = |R|\, e^{-j\theta_V} = \frac{\varepsilon_r \sin(\theta) - \sqrt{\varepsilon_r - \cos^2(\theta)}}{\varepsilon_r \sin(\theta) + \sqrt{\varepsilon_r - \cos^2(\theta)}} \tag{5}$$

$$\underline{R_H} = |R|\, e^{-j\theta_H} = \frac{\varepsilon_r \sin(\theta) - \sqrt{\varepsilon_r - \cos^2(\theta)}}{\varepsilon_r \sin(\theta) + \sqrt{\varepsilon_r - \cos^2(\theta)}} \tag{6}$$

In case where the medium boundary is a reference earth in an anechoic chamber, soil, floor in a room, etc., the value of relative permeability in a general form can be determined by the expression:

$$\varepsilon_r = \varepsilon_r' + j\varepsilon_r'' = \varepsilon_r' + j60\lambda\sigma \tag{7}$$

where λ means wave length and σ is a conductivity.

Taking into account that the resultant value of the electric field in the analyzed point is the superposition of the direct and reflected waves, the effective value of the electric field strength from the source with vertical polarization is determined by the dependence [20]:

$$\vec{\underline{E}}_V(r) = \sqrt{60EIRP} \cdot \left| \frac{f_u(\theta_1)}{r_1} \cdot \cos(\theta_1) + \frac{|R_V| \cdot f_u(\theta_2)}{r_2} \cdot \cos(\theta_2) \cdot \cos\left(\frac{2\pi}{\lambda}(r_2 - r_1) + \vartheta_V\right) \right| \tag{8}$$

where the road lengths are equal respectively:

$$r_1 = \sqrt{d^2 + (h_t - h_r)^2}, \quad r_2 = \sqrt{d^2 + (h_t + h_r)^2}$$

For a source generating electromagnetic waves with horizontal polarization, the resultant strength of the electric field in the receiving place can be calculated from equation:

$$\vec{\underline{E}}_H(r) = \sqrt{60EIRP} \cdot \left| \frac{f_u(\theta_1)}{r_1} + \frac{|R_H| \cdot f_u(\theta_2)}{r_2} \cdot \cos\left(\frac{2\pi}{\lambda}(r_2 - r_1) + \vartheta_H\right) \right| \tag{9}$$

These dependencies are correct, provided that the isotropic probe is used to measure the electric field strength.

Based on dependences (8) and (9) as well as the formulas defining the value of reflection coefficient R_V and R_H of the electromagnetic wave from the medium boundary and numerical procedures allowing for the synthesis of antenna pattern [21] the computer tool was elaborated in Mathcad program for calculating the electric field strength distribution and the equivalent power density for any antennas with known radiation characteristic, set of gain and power delivered to its terminals (Fig. 2).

The two procedures are the main part of the calculation program. The procedure presented in Figure 3 allows to determine the distribution of the electric field strength on the analyzed distance d for the selected value of the EIRP power supplied to the antenna, the signal frequency f as well as parameters characterizing the environment in which the signal is propagated.

Using the algorithm described in [21], a procedure was developed (Fig. 4) allowing the synthesis of the antenna characteristics and saving it in a numerical form. The developed procedure allows to create a 2D model of the radiation pattern of the real-world antenna with satisfactory accuracy using catalog data and measurements.

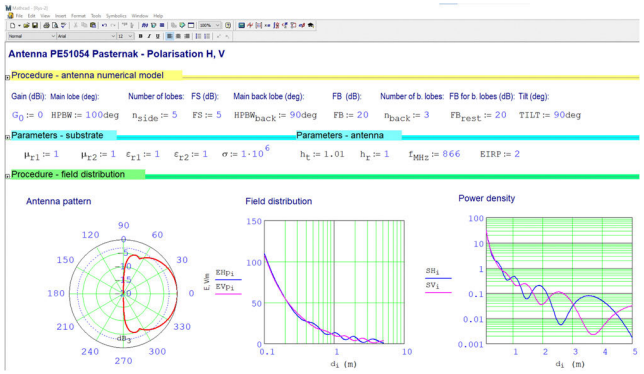

FIGURE 2. Program window for determining the distribution of electric field strength and power density for an antenna with a given characteristic, different positions of the transmitting antenna.

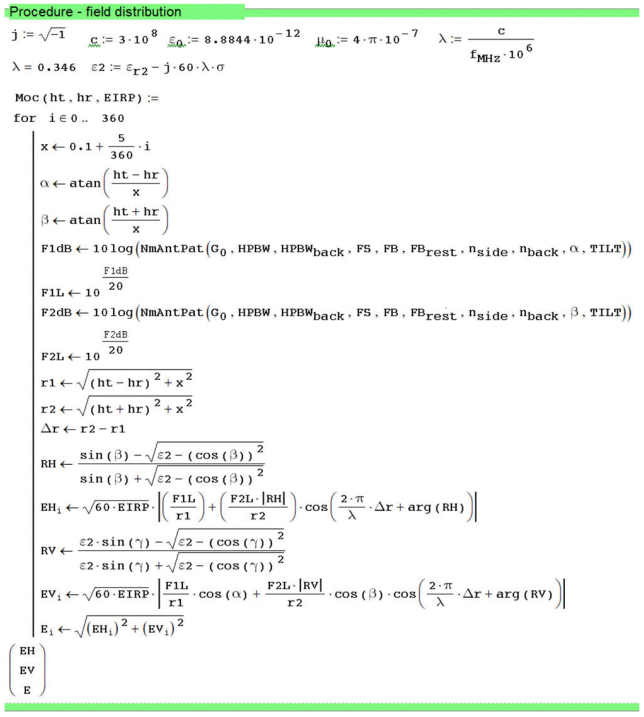

FIGURE 3. Procedure for determining the electric field strength distribution generated by the antenna at any distance d.

The elaborated tool program in the Mathcad package allows to determine of the level of electromagnetic field strength and the equivalent power density for any spatial coordination of the transmitting antenna relative to the receiving antenna (at the point of its placement) with given radiation pattern of the antenna and for any electromagnetic environment. The developed calculation procedures allow for the analysis of the distribution of these quantities in a 2D configuration.

III. PARAMETERS OF THE MODEL ANTENNA AND MATERIALS COVERING THE FLOOR OF THE ANECHOIC CHAMBER

The panel antenna with linear polarization PE51054 from Pasternak Enterprises was selected for simulations.

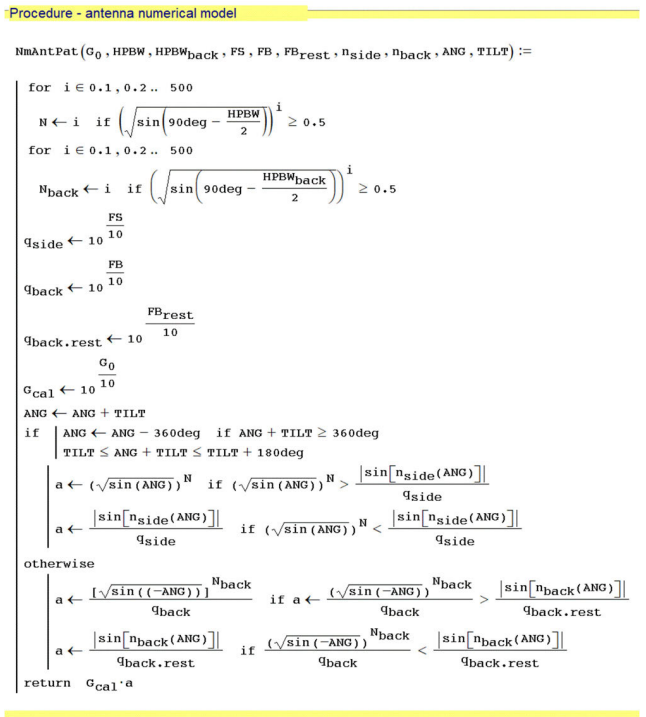

FIGURE 4. Procedure for the synthesis of the antenna radiation pattern.

This antenna enables the transmission of signals in two frequency bands: 806-960 MHz and 1710-2500 MHz with a maximum gain of 7 dBi. During the simulation tests, the level of electric field strength and power density over a distance of five meters was analyzed. The analysis was carried out for two frequencies: 865 MHz and 2.442 GHz. According to the guidelines for propagation systems operating in the frequency band from 865.1 MHz to 867.9 MHz, this frequency range is divided into three bands, where signals can be transmitted by the RFID reader with a standardized power value up to 2 W (865.6 - 867.6 MHz), 0.5 W (867.6-868) and 0.1 W (865-865.6 MHz), respectively. In case of the frequency band from 2.446 to 2.454 GHz, due to the use of the ISM public frequency band, the system can transmit a signal with EIRP power not higher than 100 mW. In the catalog note of the PE5154 antenna manufacturer, the same parameters are set in relation to the normalized radiation pattern for both frequency bands. In real world - as the measurement results indicate - the characteristics of the tested antenna are significantly different for each analyzed frequencies (Fig. 5).

To measure the radiation characteristics for the tested antenna, the system of MI Technologies was used, consisting of the Sunol Sciences ELAZ75 positioner, Sunol Sciences SC110V positioner controller and the PNA-X-N5242A vector analyzer. The received radiation patterns of the model antenna in the H and V planes were used to build their models in the MathCad program. The elaborated procedures allow modeling of standardized characteristics for any antenna.

Apart from the knowledge of the radiation pattern, to calculate the distribution of the electric field strength it is necessary

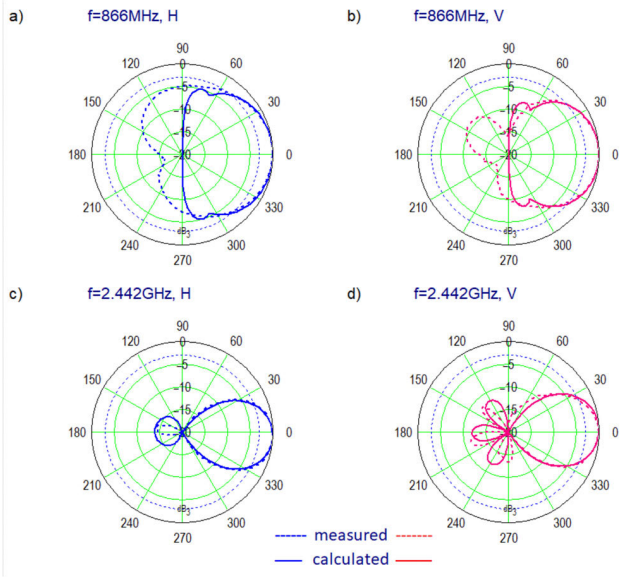

FIGURE 5. Modeled and real standardized radiation patterns of the PE51054 antenna from Pasternak Enterprises a) radiation pattern for f = 866 MHz H polarizations, b) radiation pattern for f = 866 MHz V polarizations, c) radiation pattern for f = 2.442 MHz H polarizations, radiation pattern for f = 2.442 MHz V polarizations (dotted line - real characteristics, solid line - modeled characteristics).

to know the physical parameters of the environment where the electromagnetic wave is reflected. To create free space conditions in the semi-anechoic chamber, the chamber floor was covered with ISK-030A absorbers from TDK. According to the manufacturer's note, the material is made of polyethynol foam soaked in graphite. The dielectric constant εr of this material changes as a function of frequency, however, in the case of analysis for frequencies up to 1 GHz, it can be assumed that this value is constant and has a value of 2.9. This value is determined by the dielectric constant of the carbon, which the absorber is filled. For modeling (beside the dielectric constant) it is necessary to know the conductivity of the material from which the absorbers are made. The value was taken for analysis equal to $\sigma = 0.05$ S/m. For a semi-anechoic chamber where the floor was covered with a galvanized 2 mm thick alloy sheet, the parameter values were set equal to $\varepsilon_r = 1$ and $\sigma = 107$ S/m for simulation tests.

The calculated values of the reflectance R for the electromagnetic wave at 866 MHz generated by the antenna with linear polarization are shown in Figure 6. In case of vertical wave polarization V, when the floor of the chamber is covered with absorbers for the angle of incidence 30°, the wave changes its direction (Fig. 6a). As the angle increases, the value of the electromagnetic wave coefficient decreases. After reaching the Brewster angle, the value of the reflection coefficient module increases slightly. In the case where the floor of the chamber is lined with metal, the electromagnetic wave is completely reflected irrespective of the angle of its incidence on the boundary of the medium (Fig. 6c, d).

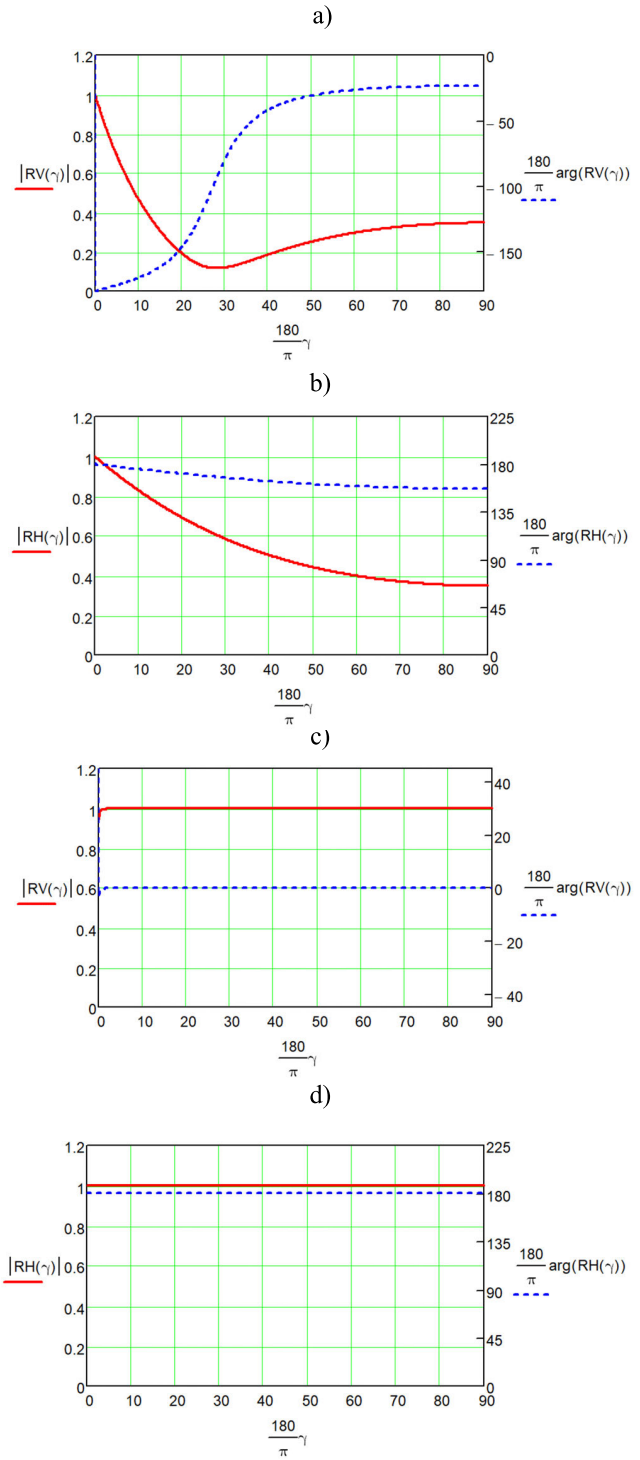

FIGURE 6. Module and argument of the reflection coefficient of the electromagnetic wave from the floor lined with absorbers (a, b) and the metal floor (c, d) for vertical polarization (a, c) and horizontal polarization (b, d) for the frequency 866 MHz.

IV. ANALYSIS OF THE ELECTRIC FIELD DISTRIBUTION GENERATED BY THE REFERENCE ANTENNA IN FREE SPACE CONDITIONS

The analysis of the electromagnetic field distribution generated by the test antenna was carried out in the anechoic

chamber. In order to create an electromagnetic space close to the free space, the chamber floor was covered with 32 absorbers IS-030A from TDK. The aim of the conducted research was to verify the propagation models allowing to determine the level of generated electromagnetic fields and the equivalent power density in conditions where the electromagnetic wave reflected from the ground wave is dispersed. For the model antenna, in the phase of simulation studies using the elaborated program, calculations of the electric field strength and power density distribution for different antenna positions in relation to the measurement probe, for selected frequency bands and different power levels sanctioned by law were carried out.

In order to facilitate the measurement process, a scanner was designed and built, which allowed for automatic movement of the measuring probe along the analyzed path over a distance of 5 m. The HI6005 isotropic probe from ETS-Lindgren was used to detect the level of the electric field strength. A set of apparatus consisting of: SMF100A microwave generator, NRP2 power meter equipped with a set of two NRP-Z21 microwave power probes from Rohde&Schwarz and a BONN 1060-100/50D power amplifier was used to generate the RF power signal. The above-mentioned equipment (in this configuration) allowed for the generation of HF signals with the required power levels in selected frequency bands, with high stability of its level.

In the first stage of the research, the situation was analyzed when the tested antenna and probe were mounted at the same height above the chamber floor surface ($h_t = h_r = 1$ m; h_t - suspension height of the tested antenna, h_r - suspension height of the measuring probe), in the state when the antenna was supplied by 2 W EIRP power for 886 MHz (Fig. 8 and 9) and 0.1 W EIRP for 2.445 GHz (Fig. 10 and 11).

The carried-out measurements in the chamber (where the floor was covered with microwave absorbers and the antenna and measuring probe were at the same height) showed that the strength of the electric field and the corresponding power density decreases in accordance with the relation for the free space. Mathematically, this dependence is described by Friis formula. Under these conditions, attenuation of the electromagnetic wave is the smallest and is called free space damping. The degree of results correlation for vertical wave polarization had a value not worse than 0.99. This value confirms that the chamber in this configuration meets the criterion of free space. When the probe is spaced within three meters from the measuring probe, the standing wave effect starts to appear (Fig. 8). This process is conditioned by the frequency of propagated signals. At 2.4 GHz, the SWR has a much lower value compared to the 866 MHz frequency.

The observed oscillation effect in the course of the electric field strength and power density for the frequency of 866 MHz is a consequence of the standing wave effect in the chamber. The longer wavelength for the 866 MHz frequency means that at the analyzed distances between the antenna and the probe, this effect is more significant than

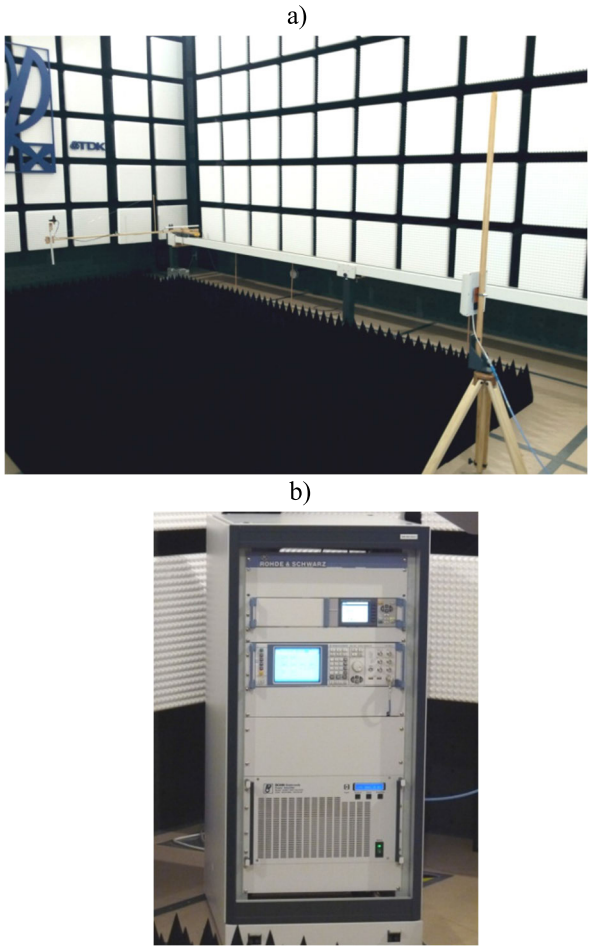

FIGURE 7. Scanner for analysis of distribution of the electric field strength and power density (a), system for generation of standard microwave signals in the EMC Laboratory at Rzeszów University of Technology (b).

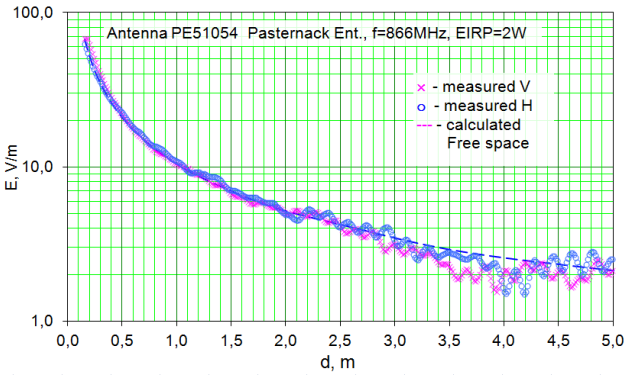

FIGURE 8. Changes of the electric field strength for the V and H polarization as a function of the distance from the UHF RFID antenna PE51054 for $h_t = h_r = 1$ m, EIRP = 2 W, f = 866 MHz.

for the 2.4 GHz frequency. This effect is due to incomplete absorption of the wave by the absorber and its dispersion on the surfaces of the absorber cones. Additionally, in the vicinity of 4 m, the greatest discrepancy between the results of calculations and measurements is observed. This is caused

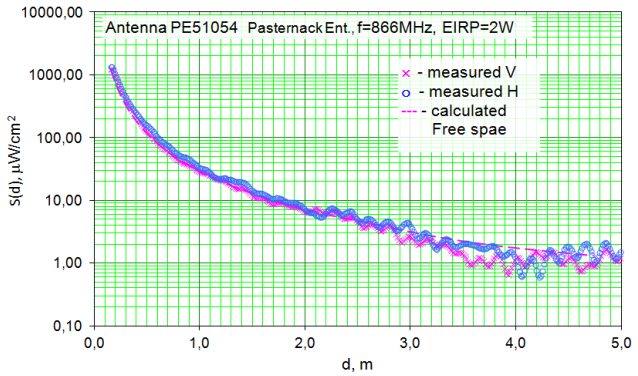

FIGURE 9. Changes in the equivalent power density for the V and H polarization as a function of the distance from the UHF RFID antenna PE51054 for $h_t = h_r = 1$ m, EIRP = 2 W, f = 866 MHz.

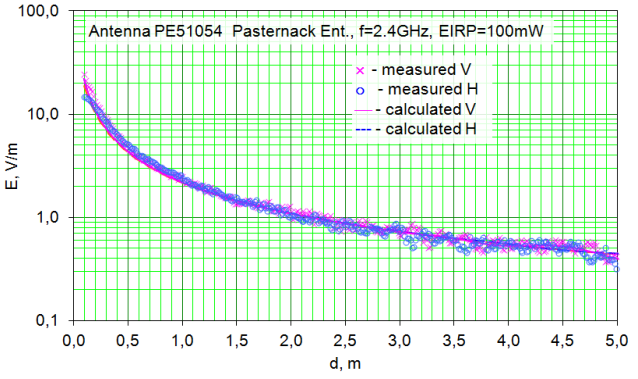

FIGURE 10. Changes of the field strength for polarization V and H as a function of the distance from the UHF RFID antenna PE51054 for $h_t = h_r = 1$ m, EIRP = 0.1 W, f = 2.445 MHz.

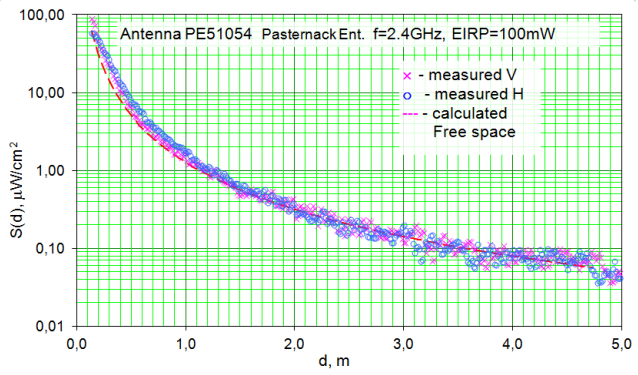

FIGURE 11. Changes in the equivalent power density for the V polarization as a function of the distance from the UHF RFID antenna PE51054 for $h_t = h_r = 1$ m, EIRP = 0.1 W, f = 2.445 MHz.

by limited size of the chamber and the effect of reflection of wave from the wall covered with ferrite plates and 0.45 m high absorbers. The tests were carried out in a TDK 3M semi-anechoic chamber 9 m long, 6 m wide and 5.8 m high.

The value of the power possible for harvesting is directly proportional to the power value delivered to the antenna. The power received when the signal propagates in the free space

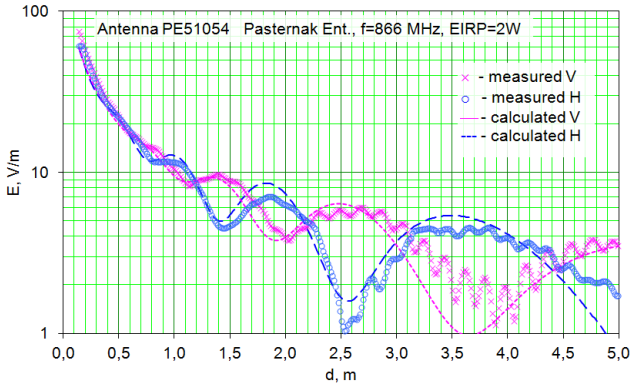

FIGURE 12. Changes of the electric field strength for the V and H polarization as a function of the distance from the UHF RFID antenna PE51054 for $h_t = h_r = 1$ m, EIRP = 2 W, f = 866 MHz.

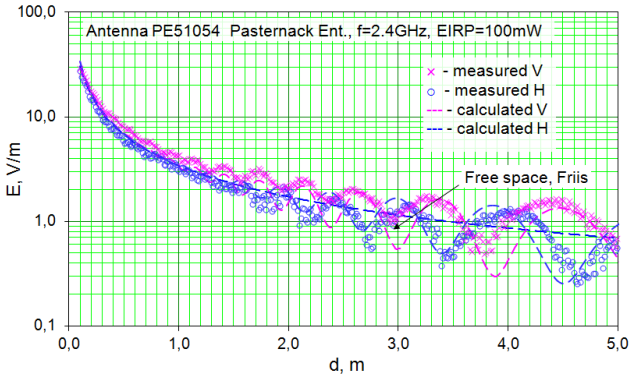

FIGURE 13. Changes of the electric field strength for the V and H polarization as a function of the distance from the UHF RFID antenna PE51054 for $h_t = h_r = 1$ m, EIRP = 0.1 W, f = 2.445 MHz.

is inversely proportional to the square of the distance from the transmitting antenna. In the case of a system in which the antenna radiates isotropic power of 2 W, the power density over a distance from 0.1 m to 5 m varies in the range from 100 μW/cm^2 to 0.1 μW/cm^2.

V. ANALYSIS OF THE ELECTRIC FIELD DISTRIBUTION GENERATED BY THE REFERENCE ANTENNA IN THE ENVIRONMENT WITH THE IDEAL SURFACE OF EARTH

The second stage of research on the possibilities of obtaining energy from antenna systems of RFID readers concerned the case where the ground plane was located on the propagation path of the electromagnetic wave. In case of an anechoic chamber, this is the floor plane covered with metal sheet. Its presence leads to the effect of a reflected wave. In this situation, the signal that is received by the isotropic probe is a superposition of waveforms reaching directly to the antenna and reflected from the floor. The two-way model has been used in the developed computational procedures. The results of the calculations (made for two frequency bands for the situation where the antenna and the probe were placed at the same height of 1 m) are presented in Fig. 12 and 13.

Analyzing the distribution of the electric and magnetic field strength for the antenna in a situation where it radiates electromagnetic waves polarized perpendicularly and parallelly to the floor plane, the effect of signal fading is observed. It is conditioned by the different length of ways on which signals reach the measuring probe, physical parameters of surfaces which reflect electromagnetic waves, frequency of propagated signals as well as parameters of the antenna. The fading effect is particularly visible in the far antenna field and becomes more prominent as the distance from the antenna increases. In places where the direct and reflected from the ground signals reached in opposite phases, the effect of mutual waveform compensation and characteristic fading is observed. The curves for vertical and horizontal polarization interleave mutually.

In the far antenna field, the change in the power level radiated by the antenna is directly proportional to the change in the level of electric field strength and the power density available in the antenna field (Fig. 14).

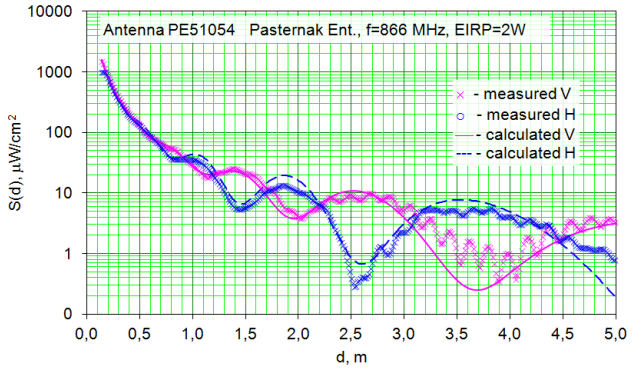

FIGURE 14. Changes in the equivalent power density for the V and H polarization as a function of the distance from the UHF RFID antenna PE51054 for $h_t = h_r = 1$ m, EIRP = 2 W, f = 866 MHz.

By changing the power value radiated by the antenna, a directly proportional change of the electric field strength value and the equivalent power density is obtained. Additionally, power changes cause situation where the curve representing the distribution of the equivalent power density changes its vertical position (Fig. 15). With this change, positions of places where fading occurs are the same.

When analyzing the results of calculations and measurements for the considered cases, a certain discrepancy can be noticed in the course of the curves. It is conditioned by the accuracy of the simulation model. The developed model takes into account the two-way effect of electromagnetic wave propagation without the standing wave effect.

When analyzing the waveforms for the 866 MHz frequency, the characteristic decay points were indicated for both horizontal and vertical polarization. Additionally, in places where the signal reaches minimum values, an increase in the level of the standing wave can be observed.

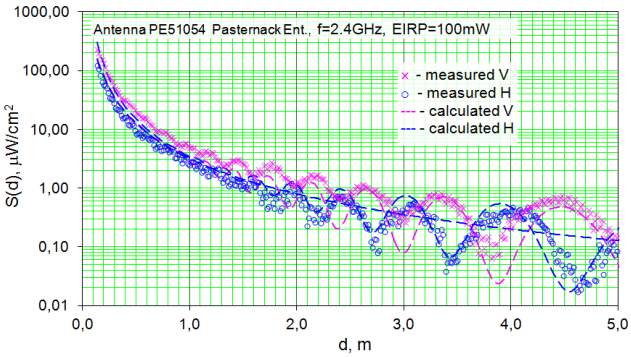

FIGURE 15. Changes in the equivalent power density for the V and H polarization as a function of the distance from the UHF RFID antenna PE51054 for $h_t = h_r = 1$ m, EIRP = 100 mW, f = 2.445 MHz.

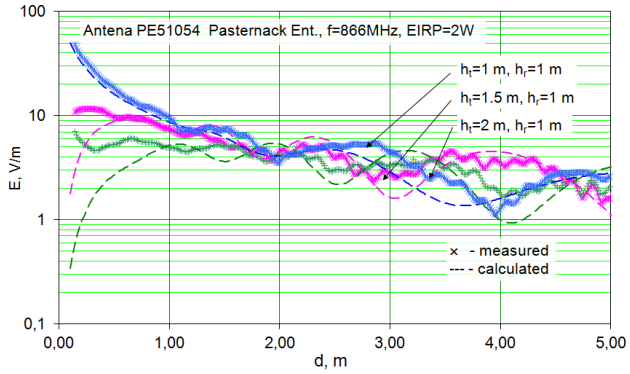

FIGURE 16. Changes in of the electric field strength for the V polarization as a function of the distance from the UHF RFID antenna PE51054 for $h_t = 1$ m and $h_r = 1, 1.5, 2$ m, EIRP = 2 W, f = 866 MHz.

At the same time, the dominance of the standing wave for vertical polarization can be observed on the measured waveforms. This is a natural consequence of the wave reflection effect on the metal floor surface. In case of horizontal polarization H, the effect of the standing wave is limited by absorbers placed on the walls of the chamber. Although it is an anechoic chamber in such a facility, the standing wave effect cannot be completely eliminated. It can only be limited to a certain level. Therefore, for such chambers, factors such as the uniformity factor FU, the standing wave factor VSWR or the normalized attenuation factor NSA in the area where the tested objects are placed are determined.

All of the analyzed situations concerned the case where tested antenna and isotropic probe were set at the same height. In the case where the transmitting and receiving antenna will be set at different heights, a significant reduction in power values near the antenna is noticeable in distributions of the equivalent power density (Fig. 16). The degree of these changes depends on the shape of the antenna characteristics. By varying the relative heights of the antenna suspensions, it is also necessary to take into account the change in the positions where the signals are lost.

VI. CONCLUSION

The main aim of the conducted research was to determine the distribution of electric field strength and power density generated by the model RFID reader antenna, dedicated to operation in the UHF frequency band. In order to demonstrate how the physical parameters of the environment where the electromagnetic wave propagates affect the distribution of the electromagnetic field generated by the antenna, the calculation procedures have been elaborated. They allow to calculate the electric field strength distribution and the equivalent power density for a given antenna radiation pattern, known environmental parameters in where the electromagnetic wave is propagated as well as any suspension height relative to ground.

In case that the environment in which electromagnetic waves are propagated is an ideal space where the wave is not reflected, the level of the electric field strength and the corresponding power density changes according to the dependence described by the Friis formula. Such conditions are possible to obtain with appropriate elevation of elements above the ground surface, floors in a non-urbanized area devoid of any elements reflecting electromagnetic waves.

The conducted simulations of electric field strength distributions and the corresponding power density showed that if the real radiation pattern for the tested antenna is taken into account in the calculations, the distribution of the generated field can be predicted with high accuracy. For RFID systems operating in the frequency range where transmission of signals with EIRP power equal to 2 W is possible, the strength of the electric field near the antenna can reach values of 80 V/m. For a distance of 2 m, this value drops to a safe value from the point of view of the field's influence on the human body equal to 7 V/m. In the case of this type of systems, the strength of the electric field was not lower than 1 V/m for a distance of five meters. On the other hand, the value of the power density in the range of variation of the relative position of the antenna in relation to the measuring probe assumed the value from 1000 μW/cm^2 to 1 μW/cm^2. In systems with a maximum power of 500 mW and 100 mW EIRP, this value is proportionally lower than the power value. Despite the lower power in the far field, at a distance of up to 5 m, the strength of the electric field varies from 7 V/m to approx. 0.5 V/m.

In order to verify the differences that were obtained between the results of calculations and measurements at this stage of the research, it is planned to use commercial tools for the analysis in the next stage, which will allow the model to take into account the limited dimensions of the measurement space and the standing wave effect.

REFERENCES

[1] Y. Kawahara, X. Bian, R. Shigeta, R. Vyas, M. M. Tentzeris, and T. Asami, "Power harvesting from microwave oven electromagnetic leakage," in *Proc. ACM Int. Joint Conf. Pervas. Ubiquitous Comput.*, New York, NY, USA, Sep. 2013, pp. 373–382.

[2] W. S. Yeoh, W. S. T. Rowe, and K. L. Wong, "Decoupled dual-dipole rectennas on a conducting surface at 2.4 GHz for wireless battery charging," *IET Microw., Antennas Propag.*, vol. 6, pp. 238–244, Jan. 2012.

[3] N. Barroca, H. M. Saraiva, P. T. Gouveia, J. Tavares, L. M. Borges, F. J. Velez, C. Loss, R. Salvado, P. Pinho, R. Goncalves, N. B. Carvalho, R. Chavez-Santiago, and I. Balasingham, "Antennas and circuits for ambient RF energy harvesting in wireless body area networks," in *Proc. IEEE 24th Annu. Int. Symp. Pers., Indoor, Mobile Radio Commun. (PIMRC)*, London, U.K., Sep. 2013, pp. 532–537.

[4] P. Soboll, V. Wienstroer, and R. Kronberger, "Stacked Yagi-Uda array for 2.45-GHz wireless energy harvesting," *IEEE Microw. Mag.*, vol. 16, no. 1, pp. 67–73, Feb. 2015.

[5] F. Musavi and W. Eberle, "Overview of wireless power transfer technologies for electric vehicle battery charging," *IET Power Electron.*, vol. 7, no. 1, pp. 60–66, Jan. 2014.

[6] L. W. Mayer, M. Wrulich, and S. Caban, "Measurements and channel modeling for short range indoor UHF applications," in *Proc. 1st Eur. Conf. Antennas Propag.*, Nice, France, Nov. 2006, pp. 6–10.

[7] M. Malajner, K. Benkič, P. Planinšič, and Ž. Čučej, "The accuracy of propagation models for distance measurement between WSN nodes," in *Proc. 16th Int. Conf. Syst., Signals Image Process.*, Chalkida, Greece, Jun. 2009, pp. 1–4.

[8] A. Lazaro, D. Girbau, and D. Salinas, "Radio link budgets for UHF RFID on multipath environments," *IEEE Trans. Antennas Propag.*, vol. 57, no. 4, pp. 1241–1251, Apr. 2009.

[9] S. R. Banerjee, R. Jesme, and R. Sainati, "A performance analysis of short range UHF propagation as application to passive RFID," in *Proc. IEEE Int. Conf. RFID*, Grapevine, TX, USA, Mar. 2007, pp. 30–36.

[10] K. Finkenzeller, *RFID Handbook*, 2nd ed. West Sussex, U.K.: Wiley, 2003.

[11] P. V. Nikitin, K. V. S. Rao, and S. Lazar, "An overview of near field UHF RFID," in *Proc. IEEE Int. Conf. RFID*, Grapevine, TX, USA, Mar. 2007, pp. 167–174.

[12] Z. Su, S.-C. Cheung, and K.-T. Chu, "Investigation of radio link budget for UHF RFID systems," in *Proc. IEEE Int. Conf. RFID-Technol. Appl.*, Guangzhou, China, Jun. 2010, pp. 164–169.

[13] H. G. Wang, C. X. Pei, and C. H. Zhu, "A link analysis for passive UHF RFID system in LOS indoor environment," in *Proc. 4th Int. Conf. Wireless Commun., Netw. Mobile Comput.*, Dalian, China, Oct. 2008, pp. 1–7.

[14] T. Stoyanova, F. Kerasiotis, A. Prayati, and G. A. Papadopoulos, "A practical RF propagation model for wireless network sensors," in *Proc. 3rd Int. Conf. Sensor Technol. Appl.*, Athens, Greece, Jun. 2009, pp. 194–199.

[15] I. Munteanu and R. Kakerow, "Simulation methodology for the assessment of field uniformity in a large anechoic chamber," *IEEE Trans. Magn.*, vol. 50, no. 2, pp. 213–216, Feb. 2014.

[16] C. Jiakui and W. Yinghong, "Simulation of the field uniformity of anechoic chamber," in *Proc. Int. Symp. Microw., Antenna, Propag. EMC Technol. Wireless Commun.*, Hangzhou, China, Aug. 2007, pp. 1349–1352.

[17] D. Mandaris, N. Moonen, S. Van de Beek, F. Buesink, and F. Leferink, "Validation of a fully anechoic chamber," in *Proc. Asia–Pacific Int. Symp. Electromagn. Compat. (APEMC)*, Shenzhen, China, May 2016, pp. 865–868.

[18] Q. Xu, L. Xing, P. Duxbury, Y. Huang, J. Noonan, and X. Zhu, "NSA simulation in semi-anechoic chamber using ray tube tracing method," in *Proc. 9th IET Int. Conf. Comput. Electromagn. (CEM)*, London, U.K., Mar./Apr. 2014, pp. 1–2.

[19] D. C. Hogg, "Fun with the Friis free-space transmission formula," *IEEE Antennas Propag. Mag.*, vol. 35, no. 4, pp. 33–35, Aug. 1993.

[20] S. J. Orfanidis. Electromagnetic waves and antennas. Rutgers University. Accessed: Jan. 4, 2021. [Online]. Available: http://eceweb1.rutgers.edu/~orfanidi/ewa/

[21] P. Jankowski-Mihułowicz, W. Lichoń, and M. Węglarski, "Numerical model of directional radiation pattern based on primary antenna parameters," *Int. J. Electron. Telecommun.*, vol. 61, no. 2, pp. 191–197, Jun. 2015.

WIESŁAW SABAT received the M.Sc. degree in electrical engineering and the Ph.D. degree from the Rzeszów University of Technology, Poland, in 1992 and 2002, respectively.

He currently works as an Assistant Professor with the Department of Electronic and Telecommunication Systems, Rzeszów University of Technology. He published over 90 scientific articles and made many expert opinions for the industry. His main research interest includes electromagnetic compatibility of civil, aerospace, and military electronic circuits, particularly in signal integrity of multiconductor transmission lines and printed circuit boards.

Dr. Sabat is an Expert of the EMC Committee of the Polish Academy of Science.

DARIUSZ KLEPACKI (Member, IEEE) received the M.Sc. degree in electrical engineering from the Rzeszów University of Technology, Poland, in 1994, and the Ph.D. degree from the Lublin University of Technology, Poland, in 2004.

He currently works as an Assistant Professor with the Department of Electronic and Telecommunication Systems, Rzeszów University of Technology. He published over 80 scientific articles and collaborates with the industry. His main research interests include electromagnetic compatibility aspects in electronic circuits as well as signal integrity in cables and transmission lines.

Dr. Klepacki was the Chair of the IEEE EMC Society-Poland Chapter (during 2015–2018 as the Vice Chair and a Secretary), from 2019 to 2020. He is a Secretary of IMAPS Poland Chapter and an Expert of the EMC Committee of the Polish Academy of Science.

KAZIMIERZ KAMUDA received the M.Sc. degree in electrical engineering from the Rzeszów University of Technology, Poland, in 1996, and the Ph.D. degree from the Łódź University of Technology, Poland, in 2006.

He currently works as an Assistant Professor with the Department of Electronic and Telecommunication Systems, Rzeszów University of Technology. He published over 80 scientific articles and collaborates with the industry. His main research interests include electromagnetic compatibility aspects in electronic circuits as well as signal integrity in communication interfaces.

Dr. Kamuda is an Expert of the EMC Committee of the Polish Academy of Science.

KAZIMIERZ KURYŁO received the M.Sc. degree in electrical engineering from the Rzeszów University of Technology, Poland, in 1996, and the Ph.D. degree from the Poznań University of Technology, Poland, in 2004.

He currently works as an Assistant Professor with the Department of Electronic and Telecommunication Systems, Rzeszów University of Technology. He published over 70 scientific articles and collaborates with the industry. His main research interests include electromagnetic compatibility aspects as well as power quality and LED lamp supply.

Dr. Kuryło is an Expert of the EMC Committee of the Polish Academy of Science.